COMPUTATIONAL MODEL OF A MAGNETIC MODULATOR FOR COPPER LASERS

C. D. Boley
University of California
Lawrence Livermore National Laboratory
Livermore, CA 94550 USA

Abstract

A numerical model of a three-stage magnetic modulator for copper lasers is described. The model follows in detail the hysteresis behavior of the magnetic switches and a transformer. The laser is treated via a simple model of field diffusion. The calculated voltage across the laser and current through the laser are shown to compare favorably with experiment.

Introduction

This paper presents simulations of a magnetic modulator which was developed to drive copper lasers used in isotope separation [1]. The circuit is shown schematically in Fig. 1; parameter values are listed in Table 1. The modulator uses a thyratron or SCR stack and three stages of magnetic compression to provide a 40-45 kV pulse to the laser at a repetition rate of 4.5 kHz. It operates at an input power of 28-36 kW. Each stage has a saturable inductor consisting of several cores made of the ferrite C/7D. There is also a 1:4 step-up transformer wound with Metglas 2605S3A.

Initially the capacitor C_0 is charged to a typical voltage of 18 kV. The magnetic switches are held in negative satutation by reset currents. All other voltages and currents are zero. After the thyratron or SCR stack closes, C_0 discharges upon C_1 with a charge time of approximately 900 ns. During this time the first magnetic switch holds off the current by presenting a large inductance to the circuit. It then saturates, allowing the energy to flow to C_2, which has a charge time of 350 ns. When the second switch saturates, the energy flows to C_3 (charge time of 90 ns), and the voltage is stepped up by a factor of 4 by the transformer. After saturation of the third switch, the voltage is transferred to the peaking capacitor (rise time of 30 ns) and then to the laser load. It then reflects back through the circuit, undergoing expansion in successive stages.

The reset circuit, not shown in Fig. 1, consists of a rod passing through each core, connected in series with a fixed voltage source, a large inductor, and a resistor.

The task of the model is to describe the detailed behavior of the voltages, currents, and fields in the modulator system. We shall see that this can be done in quite reasonable accordance with experiment.

Magnetic Model

We employ a simple core model [2] in which the magnetic field within the cores, in both the switches and the transformer, is taken to be azimuthal and to depend only on time, and the displacement current is ignored. The voltage across each core then satisfies an equation of the form

$$V(t) = L(t)\frac{dI(t)}{dt}, \tag{1}$$

where the time-dependent inductance is directly proportional to the permeability $\mu(t)$ within the core. We neglect the radial dependence of the fields, which is an effect of order 10%. The magnetic field itself evolves according to

$$\dot{B}(t) = \frac{N_w}{2\pi\bar{r}}\mu(t)\dot{I}(t), \tag{2}$$

with N_w the number of windings and $\bar{r}$ an average radius. Further details of this model are given in the Appendix.

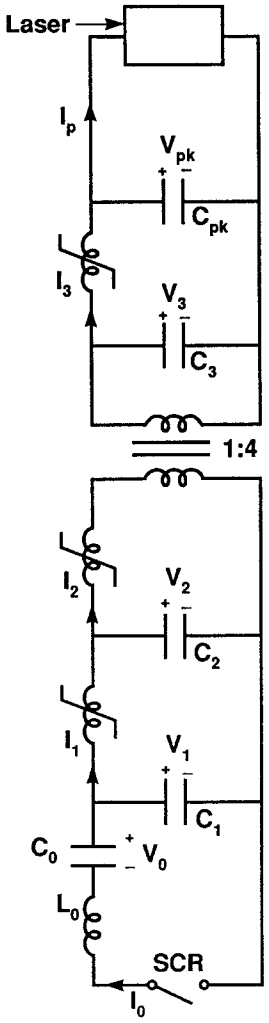

Fig. 1. Schematic modulator circuit. The reset circuit is not shown

Table 1. Modulator parameter values. Resistances listed next to capacitances are nominal ESR values.

	Stage 1	Stage 2	Stage 3	Transformer
Material	C/7D	C/7D	C/7D	2605S3A
Number of cores	10	8	10	1
Number of windings	5	2	2	4 (secondary)
Inner radius (cm)	4.57	4.57	4.57	4.45
Outer radius (cm)	7.37	7.37	7.37	7.65
Core height (cm)	1.27	1.27	1.27	10.16
Saturated L (nH)	637	67.8	450	11 (primary)
Packing factor	.95	.95	.95	.65

$C_0 = 40.5$ nF $\quad R_{C_0} = 67$ mΩ $\quad L_0 = 5$ μH
$C_1 = 40.5$ nF $\quad R_{C_1} = 67$ mΩ
$C_2 = 40.5$ nF $\quad R_{C_2} = 67$ mΩ
$C_3 = 2.5$ nF $\quad R_{C_3} = 400$ mΩ

Reset circuit parameters: $V_{re} = 12$ v, $R_{re} = 1\ \Omega$, $L_{re} = 1.2$ mH

Laser parameters: $a = 4$ cm, $\ell = 273$ cm, $L_c = 400$ nH

Report Documentation Page

Form Approved
OMB No. 0704-0188

1. REPORT DATE	2. REPORT TYPE	3. DATES COVERED
JUN 1993	**N/A**	**-**

4. TITLE AND SUBTITLE	5a. CONTRACT NUMBER
Computational Model Of A Magnetic Modulator For Copper Lasers	5b. GRANT NUMBER
	5c. PROGRAM ELEMENT NUMBER
6. AUTHOR(S)	5d. PROJECT NUMBER
	5e. TASK NUMBER
	5f. WORK UNIT NUMBER
7. PERFORMING ORGANIZATION NAME(S) AND ADDRESS(ES) **University of California Lawrence Livermore National Laboratory Livermore, CA 94550 USA**	8. PERFORMING ORGANIZATION REPORT NUMBER
9. SPONSORING/MONITORING AGENCY NAME(S) AND ADDRESS(ES)	10. SPONSOR/MONITOR'S ACRONYM(S)
	11. SPONSOR/MONITOR'S REPORT NUMBER(S)

12. DISTRIBUTION/AVAILABILITY STATEMENT
Approved for public release, distribution unlimited

13. SUPPLEMENTARY NOTES
See also ADM002371. 2013 IEEE Pulsed Power Conference, Digest of Technical Papers 1976-2013, and Abstracts of the 2013 IEEE International Conference on Plasma Science. Held in San Francisco, CA on 16-21 June 2013. U.S. Government or Federal Purpose Rights License.

14. ABSTRACT
A numerical model of a three-stage magnetic modulator for copper lasers is described. The model follows in detail the hysteresis behavior of the magnetic switches and a transformer. The laser is treated via a simple model of field diffusion. The calculated voltage across the laser and current through the laser are shown to compare favorably with experiment.

15. SUBJECT TERMS

16. SECURITY CLASSIFICATION OF:			17. LIMITATION OF ABSTRACT	18. NUMBER OF PAGES	19a. NAME OF RESPONSIBLE PERSON
a. REPORT	b. ABSTRACT	c. THIS PAGE			
unclassified	**unclassified**	**unclassified**	**SAR**	**4**	

Hysteresis properties are contained in the permeability $\mu(t)$. In the model, we employ a hysteresis theory developed by Hodgdon [3], according to which the permeability varies with B, $\dot{B}$, and H in the manner summarized in the Appendix. This theory reproduces many of the known features of hysteresis, such as loop closure near saturation, the formation of minor loops, and loop broadening with increasing $\dot{B}$. The theory requires several material parameters; those appropriate to C/7D and Metglas 2605S3A are given in the Appendix.

In previous applications [2,4], this combination of core model and hysteresis model was shown to agree satisfactorily with experiment.

We employ a simple model of the trigger switch (thyratron or SCR stack). For positive currents, it is treated as a negative 500 v source, to account for the forward drop across the switch. For negative currents, it is modeled as a 400 ohm resistor in series with the same source.

Laser Model

From the point of view of the modulator, the laser plays the role of a complicated load. For purposes of understanding modulator behavior, it suffices to treat the laser as a cylindrical plasma with constant resistivity ρ, in series with the fixed inductance L_c of the laser container. Obviously this model of the laser cannot predict detailed properties such as the optical power.

We adopt a one-dimensional model in which the electric field $E(r,t)$ points in the z direction and the magnetic field $B(r,t)$ is purely azimuthal. In the absence of displacement current, the magnetic field then satisfies a diffusion equation of the form

$$\frac{\partial B}{\partial t} = \frac{\partial}{\partial r}\frac{\rho}{\mu_0 r}\frac{\partial (rB)}{\partial r}, \tag{3}$$

with a boundary value at the radius a corresponding to the plasma current: $B(a,t) = \mu_0 I_p(t)/2\pi a$. At each instant, the electric field is given as

$$E = \frac{\rho}{\mu_0 r}\frac{\partial (rB)}{\partial r}, \tag{4}$$

and thus is not an independent dynamical quantity. The appropriate value of the resistivity, obtained by comparing a more detailed model with experiment, turns out to be approximately .3 ohm cm.

Method of Solution

It is convenient to formulate the model as a system of ordinary differential equations suitable for an ODE solver. The circuit equations are already in this form, although the hysteresis model presents extreme nonlinearities and jumps in the form of the equations.

To handle field diffusion in the plasma, we follow a conventional approach in which the magnetic field is assigned values at N nodal points distributed evenly from the center to the edge. In practice, it was found sufficient to take $N = 9$. At points 2 through $N-1$, the field then satisfies the three-point difference equation

$$\dot{B}_i = \frac{\rho}{\mu_0 \delta^2}\left[a_i^+ B_{i+1} + a_i^0 B_i + a_i^- B_{i-1}\right], \tag{5}$$

with

$$a_i^+ = \frac{i}{i-\frac{1}{2}}, \quad a_i^0 = -\frac{2(i-1)^2}{(i-\frac{1}{2})(i-\frac{3}{2})}, \quad a_i^- = \frac{i-2}{i-\frac{3}{2}}. \tag{6}$$

and δ the spacing between points. Of course B_1 is identically zero. A consistent approximation for the edge value, obtained in part by differentiating the boundary condition, is

$$\dot{B}_N = (V_{pk} - \ell E_{N-\frac{1}{2}})/(2\pi a L_c/\mu_0 + \delta\,\ell/2), \tag{7}$$

where the value of the electric field in the outermost cell is

$$E_{N-\frac{1}{2}} = \frac{\rho}{\mu_0 \delta}(a_{N-1}^+ B_N - a_N^- B_{N-1}). \tag{8}$$

Here V_{pk} is the voltage across C_{pk} and its equivalent series resistance, and ℓ is the length of the laser.

The final model, therefore, consists of a system of 15 circuit variables (5 voltages, 6 currents, and 4 core magnetic fields), along with the $N-1 = 8$ magnetic field variables in the laser. Because of the core magnetic model, this is a stiff system of ODEs. We advance it in time via the solver LSODKR, a variant of the package LSODE [5], which employs Krylov methods in numerical iterations. The solver also has root-finding capabilities which are used in transitions between branches of the hysteresis curves.

Results

After the voltage pulse is compressed and reflects back to C_0, a recovery system stores energy for the next pulse. Since this system is not treated by the model, simulations are stopped when the voltage across C_0 reaches a minimum. This occurs about 2.6 μs after the thyratron/SCR is fired.

Figure 2 shows calculated voltage waveforms for C_0, C_1, and C_2 during this interval. As one would expect, the 900 ns falloff in voltage across C_0 is matched very closely by the rise across C_1. After the first magnetic switch fires, the fall across C_1 (350 ns) is matched by the rise across C_2. After the second switch fires, the voltage is transferred from C_2 to C_3 in 90 ns. Note that, after compression, the waveforms expand as the energy reflects back to C_0. These features are in excellent agreement with expectations based on the design of the compression system.

The calculated hysteresis behavior of the three magnetic switches is shown in Figures 3, 4, and 5. Since successive stages experience increasingly higher field frequencies, the B-H loops broaden in width and develop minor loops. The widths, as measured at two-thirds the saturation value of B, are 160 At/m, 260 At/m, and 520 At/m in the respective stages. All three stages saturate twice in the positive sense. In stage 1 the second saturation occurs outside the plotted domain, but in the other two stages the loop corresponding to the second saturation is visible. The dissipated hysteresis powers are 175 W, 270 W, and 710 W, respectively.

The voltage across the laser is depicted in Fig. 6. Note that it peaks at 37 kV, drops within 90 ns to a minimum of -37 kV, and then slowly rings down with a period of about 240 ns. This behavior agrees quite well with the measured voltage trace [6], except that

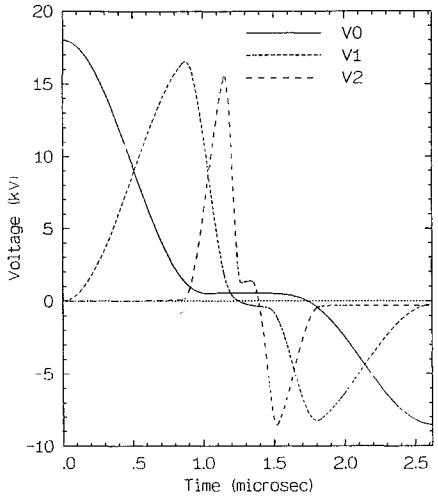

Fig. 2. Voltages across C_0, C_1, and C_2.

the latter shows somewhat less dissipation. The measurement also reveals an initial leakage, which could be modeled, if desired, by placing a capacitor across the third stage switch.

Figure 7 shows the current through the laser. The calculated current peaks at 37 kA and then rings down. The measured waveform reaches a maximum of about 60% of the calculated value, but there may be a substantial experimental error in this region. Model and experiment are reasonably close in the subsequent decay.

Finally, Figure 8 shows the calculated electric field in the laser as a function of time, at three radial locations. The field is largest near the edge, reaching a maximum of 38 v/cm, then decays as it diffuses inward.

Conclusions

These simulations show that the modulator system can be modeled with quite reasonable accuracy. The code has served as a useful guide in understanding circuit behavior and in the design of possible modifications to the device.

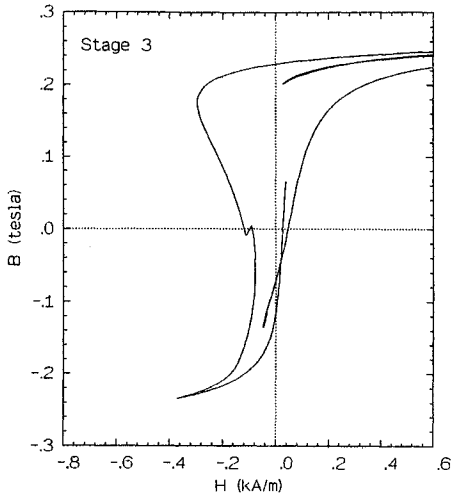

Fig. 5. Hysteresis loop of third magnetic switch.

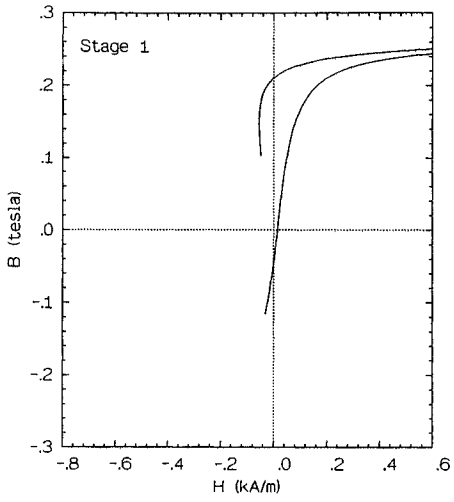

Fig. 3. Hysteresis loop of first magnetic switch.

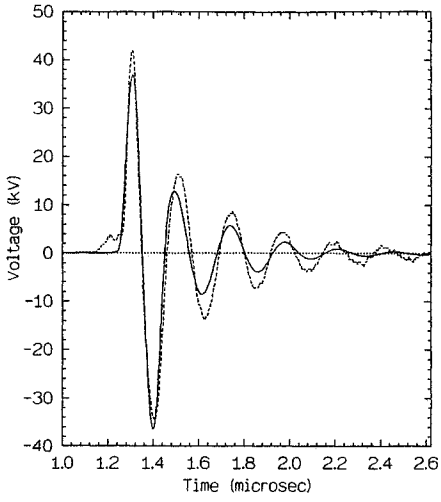

Fig. 6. Voltage across laser. The dotted line indicates Chang's data.

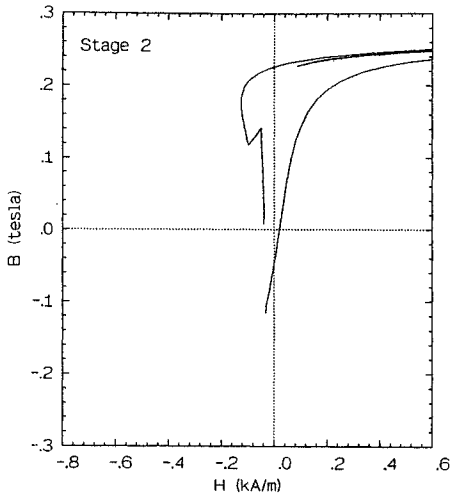

Fig. 4. Hysteresis loop of second magnetic switch.

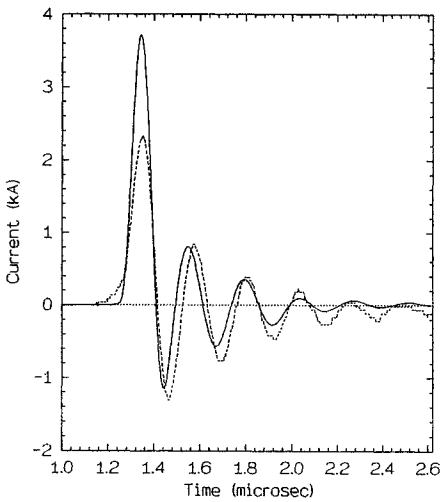

Fig. 7. Laser current. The dotted line indicates Chang's data.

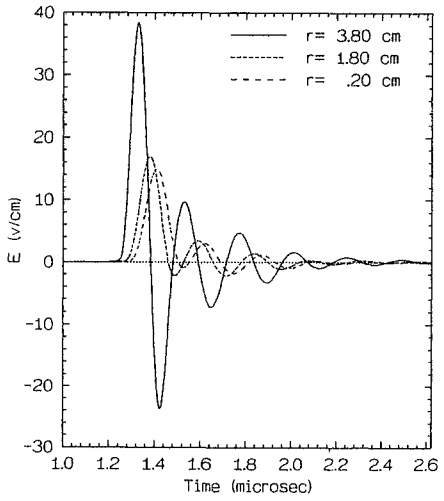

Fig. 8. Electric field in laser, at three radii.

Acknowledgments

The author is indebted to D. G. Ball, J. J. Chang, E. G. Cook, W. A. Molander, and B. E. Warner for discussions.

This work was performed under the auspices of the U.S. Department of Energy by Lawrence Livermore National Laboratory under contract No. W-7405-Eng-48.

Appendix: Details of Core Magnetic Model

Neglecting the radial dependence of the fields, the time-dependent inductance of a core is [2]

$$L(t) \approx \frac{N_w^2 h}{2\pi} \ln\left(\frac{r_{out}}{r_{in}}\right) \mu(t). \tag{A1}$$

where h is the height of a core, N_w is the number of windings, and r_{in} and r_{out} are the inner radius and outer radius, respectively. The time derivative of the magnetic field, Eq. (2), is obtained by combining the constitutive relation $\delta B = \mu \delta H$ with Ampere's law. The appropriate average radius is $\bar{r} = (r_{out} - r_{in})/\ln(r_{out}/r_{in})$.

For convenience, we collect here the needed elements of the Hodgdon theory of hysteresis [3]. The permeability varies with B, $\dot{B}$, and H according to

$$\mu(B, H, \dot{B}) = \{\alpha \,\mathrm{sign}(\dot{B})[f(B) - H] + g(B, \dot{B})\}^{-1}, \tag{A2}$$

where α is a constant and f and g are functions particular to the magnetic material. The dependence of the permeability on the sign of $\dot{B}$ leads to hysteresis. The material functions f and g have the form

$$f(B) = \begin{cases} A_1[\tan(A_2 B)]^p + f_{ex} B, & 0 \le B \le B_b; \\ A_1[\tan(A_2 B_b)]^p + f_{ex} B_b + (B - B_b)/\mu_s, & B > B_b; \\ -f(-B), & B < 0; \end{cases} \tag{A3}$$

$$g(B, \dot{B}) = \begin{cases} f'(B)\Big[1 - A_3\, c(\dot{B}) \exp\Big(-\dfrac{A_4|B|}{B_{cl} - |B|}\Big)\Big], & \text{if } |B| < B_{cl}; \\ f'(B), & \text{otherwise.} \end{cases} \tag{A4}$$

The rate dependence is governed by $c(\dot{B})$, which is given by

$$c(\dot{B}) = \begin{cases} 1 + c_1|\dot{B}|, & |\dot{B}| < \dot{B}_1; \\ 1 + c_1\dot{B}_1 + c_2(|\dot{B}| - \dot{B}_1), & \dot{B}_1 \le |\dot{B}| \le \dot{B}_2; \\ 1 + c_1\dot{B}_1 + c_2(\dot{B}_2 - \dot{B}_1) + c_3(|\dot{B}| - \dot{B}_2), & \text{otherwise.} \end{cases} \tag{A5}$$

The values of the constants for C/7D are (mks units):

$B_{cl} = .25$	$A_1 = 39.36$	$c_1 = 1.1 \times 10^{-6}$	$\dot{B}_1 = 4.2 \times 10^6$
$B_b = .2596$	$A_2 = 5.984$	$c_2 = 4.8 \times 10^{-6}$	$\dot{B}_2 = \infty$
$f_{ex} = 0$	$A_3 = -.5579$	$c_3 = \ldots$	$\dot{B}_3 = \ldots$
$p = 1$	$A_4 = .01043$	$\mu_s = \mu_0$	$\alpha = 10$

in which c_3 and $\dot{B}_3$ are not needed since only the first two branches of $c(\dot{B})$ are used. For Metglas 2605S3A, the constants are:

$B_{cl} = 1.4$	$A_1 = .08734$	$c_1 = 4.455 \times 10^{-4}$	$\dot{B}_1 = 1.1 \times 10^5$
$B_b = 1.45$	$A_2 = 1.0778$	$c_2 = 7.868 \times 10^{-5}$	$\dot{B}_2 = 3.3 \times 10^6$
$f_{ex} = .7958$	$A_3 = -8.944$	$c_3 = 5.833 \times 10^{-6}$	$\dot{B}_3 = 8.7 \times 10^6$
$p = 2$	$A_4 = .2770$	$\mu_s = .9324\mu_0$	$\alpha = 10$

References

[1] E. G. Cook et al., "High Average Power Magnetic Modulator for Copper Lasers," Proc. Eighth IEEE International Pulsed Power Conference, San Diego, CA, June 1991, p. 537.

[2] C. D. Boley and M. L. Hodgdon, "Model and Simulations of Hysteresis in Magnetic Cores," IEEE Trans. Magnetics **25**, 3922 (1989).

[3] M. L. Hodgdon, "Applications of a Theory of Ferromagnetic Hysteresis," IEEE Trans. Magnetics **24**, 218 (1988); M. L. Hodgdon, "Mathematical Theory and Calculations of Magnetic Hysteresis Curves," IEEE Trans. Magnetics **24**, 3120 (1988).

[4] C. D. Boley, "Simulations of a Magnetic Pulse Compressor," Proc. Eighth IEEE International Pulsed Power Conf., San Diego, CA, June 1991, p. 704.

[5] A. C. Hindmarsh, "ODEPACK, a Systematized Collection of ODE Solvers," in Scientific Computing, R. S. Stepleman et al. (eds.), North-Holland, Amsterdam, 1983 (Vol. I of IMACS Transactions on Scientific Computing), pp. 55–64.

[6] J. J. Chang, private communication.